

Gamma-Ray Bursts: Jets and Energetics

D. A. Frail^{a*}

^aNational Radio Astronomy Observatory, Socorro, NM 87801 USA

The relativistic outflows from gamma-ray bursts are now thought to be narrowly collimated into jets. After correcting for this jet geometry there is a remarkable constancy of both the energy radiated by the burst and the kinetic energy carried by the outflow. Gamma-ray bursts are still the most luminous explosions in the Universe, but they release energies that are comparable to supernovae. The diversity of cosmic explosions appears to be governed by the fraction of energy that is coupled to ultra-relativistic ejecta.

1. Jet Signatures in Gamma-Ray Bursts

In hindsight, since jets are a natural outcome of most high energy phenomena, they should have been expected in gamma-ray bursts (GRBs). While there had been some early indications that relativistic outflows from GRBs might not be isotropic [1,2], the real impetus for invoking jets came from the “energy crisis” brought on by the spectacular GRB 990123 [3]. On a timescale of order 80 s, the isotropic energy released in gamma-rays $E_{iso}(\gamma)$ from this burst approached the rest mass energy of a neutron star! If GRB outflows were not isotropic but instead were collimated into jets with an opening angle θ_j then they would only radiate into a fraction $f_b = (1 - \cos \theta_j) \cong \theta_j^2/2$ of the celestial sphere [4,5]. Thus the true gamma-ray energy released E_γ would be smaller than $E_{iso}(\gamma)$ by the same factor, i.e. $E_\gamma = f_b \times E_{iso}(\gamma)$.

The characteristic signature of a jet-like outflow at optical and X-ray wavelengths is an achromatic break at a time t_j in the power-law decay of the light curves (Fig. 1), in which the exponent α (defined by $F_\nu \propto t^\alpha$) steepens by $\Delta\alpha \sim 1$ [5]. At radio wavelengths, in which the emission is initially produced by electrons radiating below the peak of synchrotron spectrum ν_m , a jet break is expected initially to produce only a shallow power-law decay (e.g. $t^{-1/3}$ to t^0) of the light curve until a time when ν_m passes through the

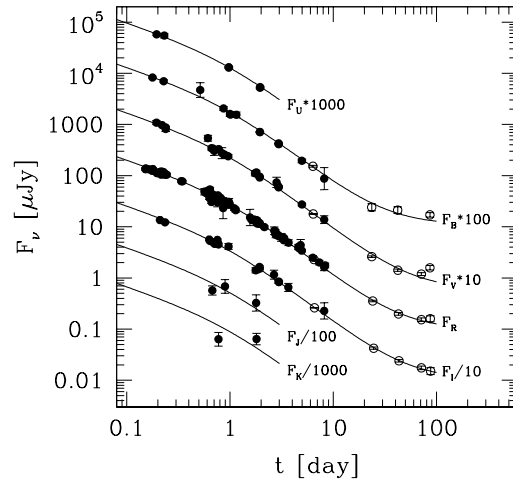


Figure 1. *The UVBRIJK band lightcurves of GRB 010222. The fits to the data are made with a broken temporal power law function added to a constant host galaxy component. The break in the light curves occurs at $t_j=0.93$ d. From [8].*

radio band. Thereafter, if the expansion remains relativistic, the power-law decay index will be the same as the optical and X-ray (i.e. $\alpha \sim -2$). GRB afterglow measurements of the degree of polarization and the polarization angle can provide a powerful diagnostic for jets [6,7], but the observations to date have been ambiguous.

The origin of this sharp break at t_j is due to two effects. The first is a purely geometric transition that occurs when the Lorentz factor Γ drops below θ_j^{-1} , and the observer begins to see the edge of the jet [4]. A second effect that may become im-

*The NRAO is a facility of the National Science Foundation operated under cooperative agreement by Associated Universities, Inc.

portant after t_j is a dynamical transition in which the jet outflow switches from a pure radial outflow to a laterally spreading jet component. With some basic understanding of the jet dynamics, a measurement of t_j and redshift z yields an estimate of θ_j and hence E_γ . Readers who wish to learn more about the practical difficulties in estimating t_j and possible systematic effects should review [9,10,11] and references therein.

2. A Standard Energy Reservoir for GRBs

In 2001 [9] we compiled all known bursts with z and t_j measurements (or limits) and derived their θ_j values using the uniform jet model [5]. The distribution of t_j ranged from 1 to 25 d, while the derived θ_j values ranged from 2.5° to 17° , with a mean of about 3.6° . One immediate implication, if GRBs are beamed to only a fraction of the sky, is that the *true* GRB rate is a factor of $\langle f_b^{-1} \rangle \sim 500$ times the *observed* rate. Thus the prompt gamma-rays which defines the GRB phenomenon is not observable by us for the vast majority of bursts. For evidence of these off-axis explosions we must look for “orphan afterglows” at optical and radio wavelengths [12,13,14].

An even more remarkable result is that the isotropic gamma-ray energy $E_{iso}(\gamma)$, which spans three orders of magnitude from $\sim 10^{51}$ erg to $\sim 10^{54}$ erg (Fig. 2), collapses into a narrow distribution of E_γ once the geometric corrections are applied. As shown in the bottom panel of Fig. 2, E_γ clusters around 5×10^{50} erg, with a $1-\sigma$ multiplicative factor of only two. This constancy of the product $E_{iso}(\gamma) \times \theta_j^2$ implies that the broad distribution of gamma-ray luminosity (and fluence) which has been observed is due in large part to the diversity in jet opening angles.

This clustering of E_γ has been recently confirmed by an improved analysis of a larger sample of bursts [11]. One weakness of the earlier work [9] was that it adopted a circumburst density $n_o = 0.1 \text{ cm}^{-3}$ for all bursts. With more precise photometric data and the increasing sophistication of afterglow modeling, the true range of n_o is $0.1 \text{ cm}^{-3} \lesssim n_o \lesssim 30 \text{ cm}^{-3}$ with a canonical value of 10 cm^{-3} [15]. The new result, shown in Fig. 3, gives a mean geometry-corrected energy

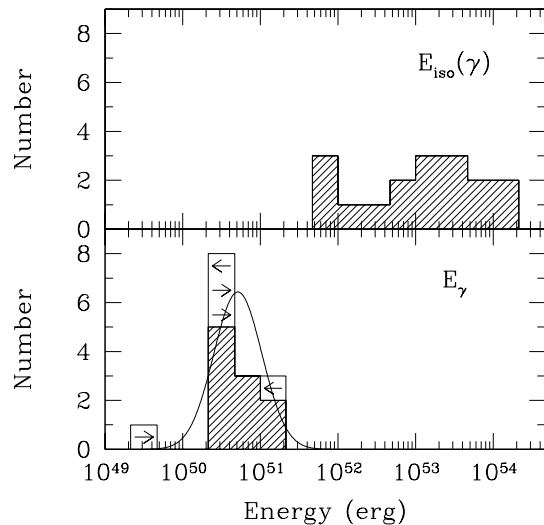


Figure 2. *The distribution of the isotropic gamma-ray burst energy of GRBs with known redshifts (top) versus the geometry-corrected energy for those GRBs whose afterglows exhibit the signature of a non-isotropic outflow (bottom). The mean isotropic equivalent energy $\langle E_{iso}(\gamma) \rangle$ for 17 GRBs is 1.1×10^{53} erg, while the mean geometry-corrected energy $\langle E_\gamma \rangle$ is 5×10^{50} erg. Arrows indicate upper or lower limits. A circumburst density $n_o = 0.1 \text{ cm}^{-3}$ has been assumed. From [9].*

$\langle E_\gamma \rangle$ of 1.33×10^{51} erg, with a $1-\sigma$ multiplicative factor of about two. The $2.7\times$ increase in $\langle E_\gamma \rangle$ over the early value is almost entirely due to the use of realistic n_o estimates.

The sharply peaked $\langle E_\gamma \rangle$ distribution has prompted suggestions that GRBs are “standard candles” and could therefore have cosmographic applications. The scatter in E_γ is too small to place meaningful constraints on cosmological parameters [11]. Moreover, the lack of local calibrators to pin down the true E_γ implies that the distribution of E_γ at higher redshifts only probes the shape of the cosmological Hubble diagram. Energy diagrams like Fig. 3 are far more useful for identifying potential sub-classes by their deviant energies. Note that $\sim 10\text{-}20\%$ of long-duration bursts are under-energetic in gamma-ray energies. We will return to this point in §5.

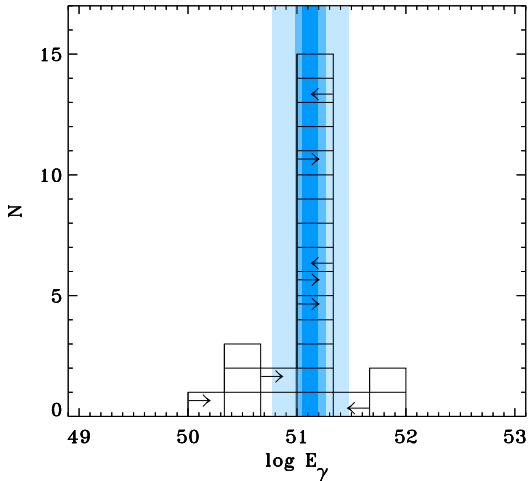


Figure 3. The distribution of geometry-corrected energies with a mean $\langle E_\gamma \rangle = 1.3 \times 10^{51}$ erg, a one-time sigma-clipped error of $\sigma = 0.07$ dex. Bands of 1, 2, and 5 σ about the standard energy are shown. There are at least five identifiable outliers, more than 5σ from the mean. From [11].

3. The Kinetic Energy of GRB Afterglows

The narrow $\langle E_\gamma \rangle$ distribution is puzzling, so it would be useful to have independent check on this result. So far we have used the gamma-ray energy as a proxy for the energy released by the GRB explosion. However, only a fraction is radiated, while the rest is carried away by the kinetic energy in the outflow². Particle acceleration occurring in this relativistic shock gives rise to long-lived afterglow emission at X-ray, optical and radio wavelengths [16]. Thus with a suitable broadband model that describes the dynamics of jet/circumburst interaction and calculates the expected synchrotron and inverse Compton emission, all the relevant quantities (E_k , n_o , and θ_j) can be calculated [17,18,19]. Although high quality, panchromatic datasets are rare and the validity of some of the underlying model assumptions have yet to be fully tested [20], the derived values of E_k range from 10^{50} to 3×10^{51} erg [15].

²The full GRB energy budget likely contains a significant amount of energy in neutrinos and gravitational waves, i.e. $E_{tot} = E_\nu + E_{grav} + E_\gamma + E_k$. The early afterglow phase may also radiate away some additional energy.

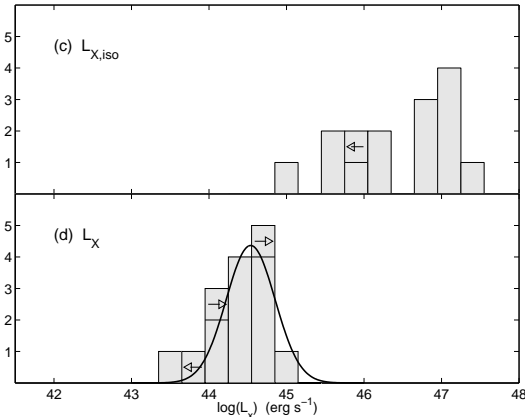


Figure 4. The distribution of the isotropic X-ray luminosity measured at 10 hrs after the burst (top) versus the geometry-corrected X-ray luminosity (bottom). The narrowing of this distribution implies that the kinetic energy in the outflow is also approximately constant. From [23].

A simpler approach is to exploit the fact that the flux density above the synchrotron cooling frequency ν_c is proportional to the energy per unit solid angle and the fraction of the shock energy carried by electrons ϵ_e [21,22]. The advantage of this method is that it is insensitive to the density of the circumburst medium or any other microphysics in the shock, provided that the emission is predominantly synchrotron. Thus X-ray afterglows, which radiate above ν_c on timescales of several hours after the burst, yield the product of $\epsilon_e \times E_k$, once θ_j is known. This approach was recently carried out on a sample of X-ray afterglows using θ_j values from [11]. The results, summarized in Fig. 4, show the dramatic narrowing of the X-ray luminosity L_X as the geometric corrections are applied [23]. Although this method does not give E_k directly, the strong clustering of L_X does imply that GRB explosions have a near standard kinetic energy yield.

There is one method for estimating E_k that does not require that we know the geometry of the outflow. At sufficiently late times the relativistic blast wave becomes sub-relativistic [1,24]. For kinetic energies of 10^{51} erg and circumburst densities of 1 cm^{-3} this occurs on a timescale of order 100 d (Fig. 5), and it can be recognized by a

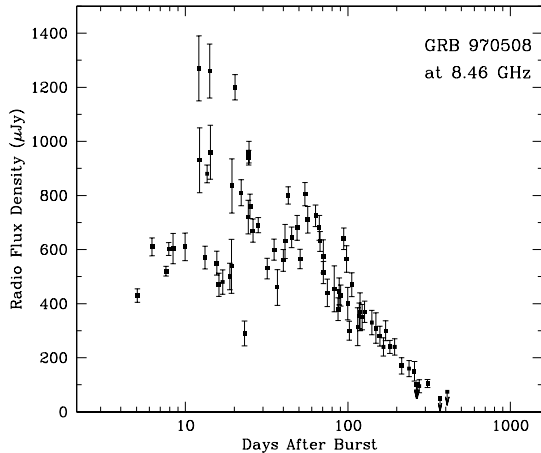


Figure 5. *Radio light curve of GRB 970508. The rapid fluctuations seen at early times are due to interstellar scintillation. At late times ($t > 100$ d) the behavior of the light curve is consistent with a quasi-spherical fireball expanding sub-relativistically. This allows true calorimetry of the explosion to be carried out, yielding $E_k \sim 5 \times 10^{50}$ erg. From [26].*

flattening of the light curves compared to a jet in the relativistic regime [25]. After this time the dynamical evolution of the shock is described by the Sedov-Taylor solutions rather than the relativistic formulation and the outflow is expected to be quasi-spherical. This method allows us to do true calorimetry of the explosion, permitting not only the energy to be inferred but also the circumburst density, the magnetic field and the size of the fireball. The radius can be checked for consistency with the equipartition radius and the interstellar scintillation radius. This method has been used for GRB 970508 [26] and for GRB 980703 (Berger, *priv. comm.*), yielding $E_k \sim 5 \times 10^{50}$ erg, in agreement with other estimates.

4. Jet Geometry: Uniform vs Universal

The jet model adopted above assumed a uniform distribution of energy (and Lorentz factor) per unit solid angle across the face of the

jet, which quickly drops to zero when the observer’s viewing angle exceeds the opening angle. Although this simple jet geometry provides a straightforward way to estimate θ_j from t_j , it is unlikely to be correct in practice. In collapsar simulations of a relativistic jet propagating through the stellar progenitor, the Lorentz factor of the ejecta is high near the rotation axis, but decreases off axis [27]. This has prompted an alternative model in which GRBs have a structured jet configuration with the energy per unit solid angle varying as $\epsilon(\theta) \propto \theta^{-k}$, where θ is a viewing angle that increases away from the jet symmetry axis. In this model all jets have the same universal “beam pattern” and the breaks in afterglow light curves at t_j are a viewing angle effect.

Apart from its physical appeal, there are a number of distinct advantages to the universal jet model. Well-known correlations between gamma-ray luminosity, variability, spectral lag, and jet break time [28,29,30] can be understood in the context of this structured jet [31,32]. Moreover, the near-constant energy result in §2 can be preserved if there exists a quasi-universal jet configuration for all GRBs with $k \simeq 2$ [33,34]. It is worth noting in this context that a prescient paper [35] had earlier predicted both a quasi-universal jet configuration and a standard energy yield for GRBs.

We have recently argued [36] that a universal structured jet can also predict the observed distribution of jet angles θ_j . One might naively expect that the number $dn(\theta)/d\theta$ of bursts with angle in the interval $d\theta$, around θ would be proportional to θ_j , the observers viewing angle. This implies that most bursts should have a large angle, contradicting the observed distribution (Fig. 6) which shows a peak near 6° , a deficit of narrow jets and a falloff in the number of wide-angle jets, characterized by [9] as a power-law $dn/d\theta \propto \theta_j^{-2.5}$. However, this argument ignores the fact that bursts with small θ are brighter by a factor of θ^{-2} , and therefore can be seen (in a Euclidian universe) up to a distance θ^{-1} farther, which contains a volume larger by a factor of θ^{-3} . Cosmological effects further limit the volume at large redshifts, producing a cutoff in the number of the narrowest jets. When these effects are accounted for, they

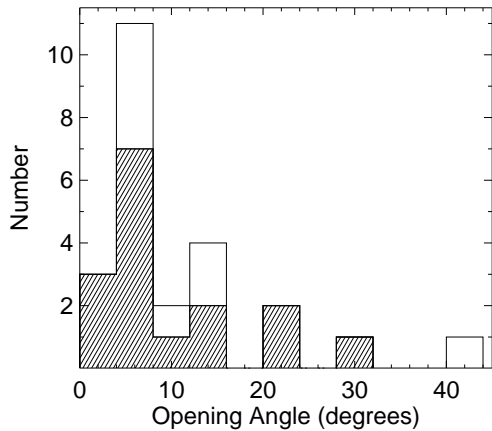


Figure 6. *The distribution of observed jet angles θ_j formed from data taken from [11]. Hatched squares represent true θ_j values, while unfilled squares are upper or lower limits on θ_j . The structured jet model predicts a distribution of θ_j which is consistent with what is observed [36].*

reproduce the observed distribution reasonably well and provide specific predictions for future, more sensitive, gamma-ray experiments.

Despite the indirect evidence in favor of a universal structured jet it remains far from proven. The resolution of this issue is an important one since it affects estimates for the true GRB event rate and the total energy, and it is crucial for possible unification schemes of cosmic explosions (e.g. [37]). Fortunately, there are a number of ways to discriminate between the uniform and structured jet paradigms. As in the case of the opening angle distribution $dn(\theta)/d\theta$, the structured jet model makes specific predictions for the slope of the GRB luminosity function which are best tested in future experiments [33,34]. Using analytic and numerical hydrodynamic modeling, detailed predictions have been made for Gaussian and power-law jet profiles (in both Γ and ϵ) [33,38,39,40,41]. The light curves produced by a jet in which *both* Γ and ϵ vary as the inverse square of the angular distance from the jet symmetry axis are almost indistinguishable from a uniform jet. With other parameter values significant departures from the familiar bro-

ken power-law are predicted, including variations in the sharpness of the break with viewing angle and a flattening of the light curve before and after the jet break time. Although some quantitative comparisons have been made [41], we currently lack well-sampled photometry around t_j for a sufficient sample of bursts to properly constrain jet structure. Polarization studies of afterglows show considerable promise in this regard. Preliminary calculations [42,38] predict a peak in the degree of polarization near t_j and (unlike the uniform jet) predict no variation in the polarization angle with time. The recent measurement of a time-variable position angle from the polarized emission of GRB 021004 has been used to argue against the structured jet model [43]. Since there was no corresponding break in the light curves on the same timescale as the position angle variations, we consider this issue unsettled.

5. Cosmic Explosions: Quality vs Quantity

As noted in §2 there are true low energy outliers in the distribution of E_γ (Fig. 3). This includes events like GRB 980519 and GRB 980326 which were classified as fast-faders (f-GRBs) based on the steep decline of their optical light curves ($F_\nu \propto t^{-2}$) at early times. The archetype of the f-GRB sub-class is GRB 030329 which exhibited a clear jet break at optical (and X-ray) wavelengths at $t_j = 0.55$ d [44], implying $E_\gamma \simeq 5 \times 10^{49}$ erg - significantly below the mean $\langle E_\gamma \rangle = 1.3 \times 10^{51}$ erg. The peculiar GRB 980425, associated with the Type Ic SN 1998bw [45,46], may define another possible sub-class of nearby ($d < 100$ Mpc), low-luminosity events that are associated with bright supernovae (S-GRBs) [47,30]. Based on its gamma-ray properties GRB 980425 was severely under-energetic with $E_{iso}(\gamma) \simeq 7 \times 10^{47}$ erg. If we are to understand this apparent diversity of cosmic explosions we must look more closely at the *total* energetics of these peculiar events.

While the X-ray and optical observations of GRB 030329 showed an early jet break ($t_j = 0.55$ d), the centimetre and millimetre light curves [48,49], contrary to expectations, continued to rise before exhibiting a break at ($t_j = 9.8$ d). We proposed a two component jet model with a

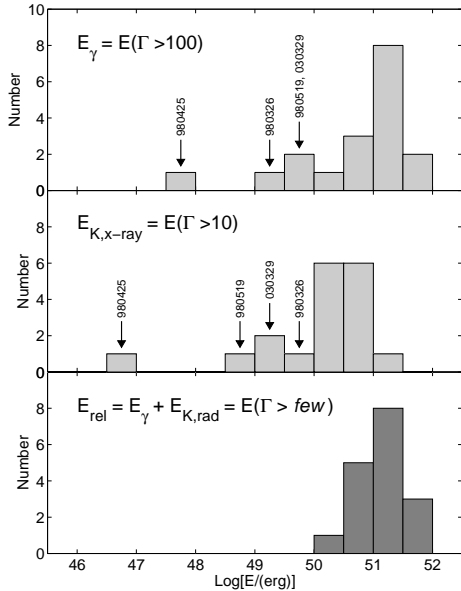


Figure 7. *Energy histograms.* The top panel shows the distribution of gamma-ray energy E_γ and the center panel shows the kinetic energy E_k inferred from X-rays (assuming $\epsilon_e = 0.1$). Both of these methods are only sensitive to ejecta with large Lorentz factors ($\Gamma > 10$). Significant outliers are labeled, including GRB 980425 and GRB 030329. If the total relativistic energy E_{rel} is derived instead (bottom panel), the dispersion narrows significantly as the energy outliers draw closer to the mean energy. This implies that cosmic explosions produce approximately the same quantity of energy, but the quality, as traced by ultra-relativistic ejecta, varies widely. From [48].

narrow angle jet ($t_{NAJ} = 0.55$ d and $\theta_{NAJ} = 0.09$ rad) which is responsible for the early afterglow, and a wide angle jet ($t_{WAJ} = 9.8$ d and $\theta_{WAJ} = 0.3$ rad) which carries the bulk of the energy in the outflow and dominates the optical and radio emission after ~ 1.5 d [48]. After accounting for this lower Lorentz factor ejecta with a wider opening angle, the total energy yield (E_γ and E_k) is more in line with estimates derived for “typical” bursts in §2 and §3. Similarly, for GRB 980425, most of the explosion energy does not appear to have been channeled into an ultra-relativistic component. An analysis of the radio

properties of SN 1998bw gives convincing evidence for a relativistic component with $\Gamma = 2-3$, and a *minimum* energy $E_k \simeq 10^{50}$ erg [46,50].

The hypothesis that emerges from this work is that cosmic explosions (e.g. S-GRBs, f-GRBs, and GRBs) all draw from a standard energy reservoir, but for reasons not currently understood, the fraction of energy coupled to ultra-relativistic energy varies. Simply put, cosmic explosions have the same *quantity* of energy, but the *quality* of that energy varies (Fig. 7).

6. Conclusions and Future Work

For the last decade or more, progress in our understanding of GRB progenitors has marched in lock step with the convergence of the GRB energy scale. By 1992 we knew from their peak flux and sky distribution that GRBs were consistent with either a cosmological population or a hitherto unseen population of sources in the halo of our Galaxy. The resulting eight orders of uncertainty in the energy scale led to a plethora of possible progenitor models [51]. With the demonstration that GRBs were cosmological [52], this initial uncertainty shrank but the isotropic gamma-ray energy still spanned three orders of magnitude – reaching $\sim 10^{54}$ erg – creating a real strain on plausible burst models.

The solution, which seems obvious only in hindsight, was to recognize that the relativistic outflows from GRBs are jet-like, not isotropic (§1). Consequently it appears that there is a near standard energy yield of $\sim 10^{51}$ erg in both the radiated and the kinetic energy of the GRB explosion (§2-3). This result is all the more remarkable when it is combined with strong evidence supporting the view that long-duration GRBs are the result of the core collapse of a massive star, aka “collapsar” [53,54]. It is convenient to think of a collapsar explosion as having two distinct equal-energy components: quasi-isotropic ejecta expanding with velocity $\Gamma \simeq 1.005$ producing the familiar radioactively powered supernova light curves, and a highly collimated flow with $\Gamma \simeq 100$ powered by synchrotron emission from electrons accelerated in the relativistic shock. This picture, however, appears to be too simple, since there

is now growing evidence that the Lorentz factor of the relativistic ejecta can vary as a function of viewing angle and from one event to the next (§4). Energy appears to be the one quantity that is (roughly) conserved throughout (§5).

By understanding the GRB energy budget we are gaining fundamental insight into the inner workings of the central engine. As we move forward studying new sub-classes of cosmic explosions, such as X-ray flashes, events with on-going energy injection [55], and bursts with distinct high-energy components [56], we would be well-served to keep calorimetry as an essential tool.

Acknowledgements. I would like to thank Ed van den Heuvel, who made it possible for me to attend this meeting and give a final farewell to *BeppoSAX* - The Little Satellite That Could. Much of the work summarized in this paper was done by my collaborators, including PhD students Edo Berger, Paul Price, and Sarah Yost.

REFERENCES

1. Waxman, E., Kulkarni, S. R., and Frail, D. A. *ApJ*, **497**, 288–293, (1998).
2. Rhoads, J. E. *A&AS*, **138**, 539–540, (1999).
3. Kulkarni, S. R., *et al.* *Nature*, **398**, 389–394, (1999).
4. Rhoads, J. E. *ApJ*, **525**, 737–749, (1999).
5. Sari, R., Piran, T., and Halpern, J. P. *ApJ*, **519**, L17–L20, (1999).
6. Ghisellini, G. and Lazzati, D. *MNRAS*, **309**, L7–L11, (1999).
7. Sari, R. *ApJ*, **524**, L43–L46, (1999).
8. Galama, T. J., *et al.* *ApJ*, **587**, 135–142, (2003).
9. Frail, D. A., *et al.* *ApJ*, **562**, L55–L58, (2001).
10. Bloom, J. S., Frail, D. A., and Sari, R. *AJ*, **121**, 2879–2888, (2001).
11. Bloom, J. S., Frail, D. A., and Kulkarni, S. R. *ApJ*, **594**, 674–683, (2003).
12. Nakar, E., Piran, T., and Granot, J. *ApJ*, **579**, 699–705, (2002).
13. Levinson, A., Ofek, E. O., Waxman, E., and Gal-Yam, A. *ApJ*, **576**, 923–931, (2002).
14. Totani, T. and Panaitescu, A. *ApJ*, **576**, 120–134, (2002).
15. Panaitescu, A. and Kumar, P. *ApJ*, **571**, 779–789, (2002).
16. Mészáros, P. *Ann. Rev. Astr. Ap.*, **40**, 137–169, (2002).
17. Harrison, F. A., *et al.* *ApJ*, **559**, 123–130, (2001).
18. Panaitescu, A. and Kumar, P. *ApJ*, **554**, 667–677, (2001).
19. Frail, D. A., *et al.* *ApJ*, **590**, 992–998, (2003).
20. Yost, S. *et al.* A Study of the Afterglows of Four GRBs: Constraining the Explosion and Fireball Model. *ApJ*, in press; astro-ph/0307056, (2003).
21. Kumar, P. *ApJ*, **538**, L125–L128, (2000).
22. Freedman, D. L. and Waxman, E. *ApJ*, **547**, 922–928, (2001).
23. Berger, E., Kulkarni, S. R., and Frail, D. A. *ApJ*, **590**, 379–385, (2003).
24. Wijers, R. A. M. J., Rees, M. J., and Mészáros, P. *MNRAS*, **288**, L51–L56, (1997).
25. Frail, D. A. *et al.* A Late-Time Flattening of Afterglow Light Curves. *ApJ* in press; astro-ph/0308189, (2004).
26. Frail, D. A., Waxman, E., and Kulkarni, S. R. *ApJ*, **537**, 191–204, (2000).
27. Zhang, W., Woosley, S. E., and MacFadyen, A. I. *ApJ*, **586**, 356–371, (2003).
28. Norris, J. P., Marani, G. F., and Bonnell, J. T. *ApJ*, **534**, 248–257, (2000).
29. Salmonson, J. D. and Galama, T. J. *ApJ*, **569**, 682–688, (2002).
30. Norris, J. P. *ApJ*, **579**, 386–403, (2002).
31. Salmonson, J. D. *ApJ*, **544**, L115–L117, (2000).
32. Ramirez-Ruiz, E. and Lloyd-Ronning, N. M. *New Astr.*, **7**, 197–210, (2002).
33. Rossi, E., Lazzati, D., and Rees, M. J. *MNRAS*, **332**, 945–950, (2002).
34. Zhang, B. and Mészáros, P. *ApJ*, **571**, 876–879, (2002).
35. Lipunov, V. M., Postnov, K. A., and Prokhorov, M. E. *Astronomy Reports*, **45**, 236–240, (2001).
36. Perna, R., Sari, R., and Frail, D. *ApJ*, **594**, 379–384, (2003).
37. Lamb, D. Q. *et al.* A Unified Jet Model of X-Ray Flashes and Gamma-Ray Bursts.

- astro-ph/0309456, (2003).
38. Salmonson, J. D. *ApJ*, **592**, 1002–1017, (2003).
 39. Granot, J. and Kumar, P. *ApJ*, **591**, 1086–1096, (2003).
 40. Kumar, P. and Granot, J. *ApJ*, **591**, 1075–1085, (2003).
 41. Panaitescu, A. and Kumar, P. *ApJ*, **592**, 390–400, (2003).
 42. Rossi, E., *et al.* Polarization Curves of GRB Afterglows Predicted by the Universal Jet Structure. astro-ph/0211020, (2002).
 43. Rol, E., *et al.* *A&A*, **405**, L23–L27, (2003).
 44. Price, P. A., *et al.* *Nature*, **423**, 844–847, (2003).
 45. Galama, T. J., *et al.* *Nature*, **395**, 670–672, (1998).
 46. Kulkarni, S. R., *et al.* *Nature*, **395**, 663–669, (1998).
 47. Bloom, J. S., *et al.* *ApJ*, **506**, L105–L108, (1998).
 48. Berger, E. *et al.* A Common Origin for Cosmic Explosions Inferred from Fireball Calorimetry. *Nature*, in press; astro-ph/0308187, (2003).
 49. Sheth, K., *et al.* *ApJ*, **595**, L33–L36, (2003).
 50. Li, Z. and Chevalier, R. A. *ApJ*, **526**, 716–726, (1999).
 51. Nemiroff, R. J. in *Gamma-Ray Bursts, Proceedings of the 2nd Workshop held in Huntsville, Alabama*, New York: American Institute of Physics (AIP). Edited by Gerald J. Fishman, 730–734, (1994).
 52. Metzger, M. R., *et al.* *Nature*, **387**, 879, (1997).
 53. Stanek, K. Z., *et al.* *ApJ*, **591**, L17–L20, (2003).
 54. Hjorth, J., *et al.* *Nature*, **423**, 847–850, (2003).
 55. Fox, D. W., *et al.* *Nature*, **422**, 284–286, (2003).
 56. González, M. M., Dingus, B. L., Kaneko, Y., Preece, R. D., Dermer, C. D., and Briggs, M. S. *Nature*, **424**, 749–751, (2003).